46th AIAA Aerospace Sciences Meeting and Exhibit
7 - 10 January 2008, Reno, Nevada

AIAA 2008-987

Impulse Generated by a Shock Tube in a Vacuum

Yasuhiro Takashima[†] and Jiro Kasahara[‡]
University of Tsukuba, Tsukuba, Ibaraki, 305-8573, Japan

Joseph E. Shepherd[§]
California Institute of Technology, Pasadena, California, 91125

and

Ikko Funaki[**]
JAXA/ISAS, Sagamihara, Kanagawa, 229-8510, Japan

Detonation tube specific impulse increases with decreasing ambient pressure for fully-filled conditions in a sub-atmospheric environment. In the present study, we use an open-end shock tube to simulate a detonation tube and investigate the dependence of the specific impulse on the propellant fraction, i.e., partial filling, in vacuum operation. The impulse is experimentally determined by hanging the shock tube in a ballistic pendulum arrangement inside a vacuum chamber. The shock tube driver section has a fixed length of 0.1 m and is filled to 1 MPa with various gases including helium, hydrogen, nitrogen, argon, and sulfur hexafluoride. The pressure inside the vacuum chamber is 5 Pa. The shock tube had constant area and different lengths (0-1.2 m) of the open-end driven sections (extension tubes) are used to vary the fraction of gas filling the shock tube (fill fraction) between 7.8% and 100%. The specific impulse is a weak function of extension tube length but varies strongly with the gas type. Dimensional analysis is used to correlate the data and we show that similar to data from detonation tubes, it is possible to correlate specific impulse with a single parameter that takes into account the time scale for depressurization. The specific impulse is predicted using the method of characteristics ignoring two-dimensional and rarefied gas effects at the tube exit. In agreement with the experiments, the specific impulse is predicted to increase slightly with extension tube length and vary inversely with the square root of the molecular weight of the gas. The specific impulse observed for SF_6 is about 25% higher that observed for the other gases with the same extension tube lengths, indicating an effect of vibration-translational energy exchange on the exhaust velocity.

Nomenclature

A	=	cross section area of a shock tube
c_0	=	initial sound speed
F	=	non-dimensional impulse scaling function
g	=	gravitational acceleration
I	=	impulse
I_{sp}	=	specific impulse
$I_{sp}{}_*$	=	specific impulse scaling parameter
$I_{sp}(l)$	=	specific impulse of a shock tube with an extension tube of length l
L	=	non-dimensional length

[†] Graduate Student, Department of Engineering Mechanics and Energy, 1-1-1 Tennodai, Tsukuba; e0311318@edu.esys.tsukuba.ac.jp, Student Member AIAA.
[‡] Associate Professor, Department of Engineering Mechanics and Energy, 1-1-1 Tennodai, Tsukuba, Member AIAA.
[§] Professor, Aeronautics and Mechanical Engineering, MS 105-50, Member AIAA.
[**] Associate Professor, Research Division for Space Transportation Engineering, 3-1-1 Yoshinodai, Sagamihara, Member.

l = extension tube length
l_0 = shock tube length
l_w = pendulum wire length
m = pendulum mass
m_g = driver gas mass
p = pressure
p_0 = initial-fill pressure
p_w = closed-end wall pressure
$\Re$ = universal gas constant
T_0 = initial temperature
t = time
t^* = plateau time
u_∞ = final gas velocity
V = volume inside a shock tube
v_0 = initial velocity of pendulum
x = location in the x axis
γ = specific heat ratio
Δx_{max} = maximum horizontal displacement
μ = molecular weight
ρ_0 = initial-fill density

Superscripts

$\bar{}$ = experimental value

I. Introduction

A pulse detonation engine[1] (PDE) is an internal combustion engine which generates intermittent thrust and high-enthalpy burned gases by using detonation waves. Since a detonation waves will compress an initial gas in the combustor, the PDE can be operated without a mechanical compressor (or with a smaller amount of compression than a conventional gas turbine) and is potentially a simpler device than a gas-turbine or rocket engine. The PDE is being studied actively in many countries as a possible new type of an aerospace engine. This engine can either generate thrust directly as reaction motor with intermittent (pulsed) jets of combustion products or else indirectly by using intermittent detonation as a combustion chamber to drive a turbine. In the direct thrust generation mode, detonation tubes can be operated either completely or partially filled with combustion gases. The specific impulse is observed by a number of researchers[2-13] to be greater when the detonation tube is partially-filled instead of completely filled. In these "partial fill'' experiments and analysis, a portion of the detonation tube near the closed end (thrust surface) contains the combustible mixture while the remaining portion of the tube up to the open end contains an inert gas mixture, .e.g., air. The general conclusions of these studies are that an inert section will increase the specific impulse (impulse per unit mass of combustible mixture) although the total impulse decreases. Based on these studies, the use of partially-filled detonation tubes has been proposed as a technique for improving specific performance.

A number of simple models have been proposed to account for the partial filling effect but there is no consensus regarding the best way to model this effect and correlate performance. Detailed comparisons between experiments and models are complicated by the difficulties of generating an ideal detonation in a small length tube, and non-ideal process such as heat transfer losses may be significant.[14,15] Cooper and Shepherd[16, 17] and Morris[18] reported a specific impulse increment with decreasing ambient pressure for a fully-filled thrust tube, even in a vacuum. To date, only fully-filled detonation tubes have been studied in sub-atmospheric conditions.

The goal of the present study is to investigate the dependence of specific impulse on the amount of propellant (the partial fill effect) in a vacuum. Instead of a single-cycle detonation tube, we used a shock tube with a long extension tube to simplify the analysis of the gas dynamics. The shock tube with an open end is filled with high pressure gas separated the vacuum by a diaphragm. A pneumatically-activated cutter ruptures the diaphragm to initiate the gas expansion process. The unsteady expansion of the driver gas is similar to the behavior of the high-

pressure burned gas following a detonation wave in a detonation tube. Impulse is measured directly using the ballistic pendulum method inside a large vacuum chamber, and also, computed using the method of characteristics. We used helium, argon, nitrogen, hydrogen, and sulfur hexafluoride (SF_6) as the driver gases in order to examine the dependence on molecular weight and specific heat ratio. We changed the fill fraction by varying the length of the extension tubes that formed the driver section. In all cases, the extension tubes were directly open to the vacuum chamber and therefore at the vacuum condition.

Table 1 Gas species properties used in MOC and scaling analyses. P_0 = 1.0 MPa, T_0 = 300 K.

	H_2	He	N_2	Ar	SF_6
μ (g/mol)	2	4	28	40	146
γ	1.4	1.667	1.4	1.667	1.154
c_0 (m/s)	1321	1019	353	322	140
t^* (μs)	76	99	286	313	719
$I_{sp}{}^*$ (s)	95.0	61.8	25.4	19.5	12.3

II. Analysis

The ideal flow in the shock tube is one-dimensional if we ignore the diaphragm opening effects and the flow near the exit into the vacuum tank. Assuming a planar diaphragm that instantaneously ruptures, the resulting flow initially consists of a simple expansion wave in the shock tube. The expansion reflects from the closed end of the driver section and results in a non-simple region but one that is shock free. At the open end of the shock or expansion tube the flow is either sonic or supersonic. Since the entropy is uniform in the flow, it is straightforward to compute the gas motion by the method of characteristics[19] (MOC) for the cases with and without an extension tube. For our analysis, we assume that the flow in the shock tube is one-dimensional and ignore gas viscosity, heat transfer, and assumed that the ambient gas (vacuum condition) is at zero pressure. We calculate the specific impulse for each driver gas by using the method of characteristics. Molecular weight and specific heat ratio of each driver gas (argon, helium, nitrogen, hydrogen, and sulfur hexafluoride) are shown in Table 1.[20] The initial fill pressure p_0 is 1.0 MPa and the initial temperature is 300 K. In addition, the scaling of the impulse with tube dimensions and gas type can be determined by using ideas that were originally developed for modeling pulse detonation engines.

A. MOC Computation without Extension Tube

The x-t diagram with characteristic curves and the closed-end-wall pressure history p_w are shown in Fig. 1. The diaphragm at the open end is ruptured at the time t = 0, and the expansion wave propagates toward the closed end. After the diaphragm rupture, the characteristic lines of the expansion fan (the region ABC) spread from the open end. The head of the expansion wave front propagates to the closed end. Until a time $t = t^*$, the pressure at end of the shock tube

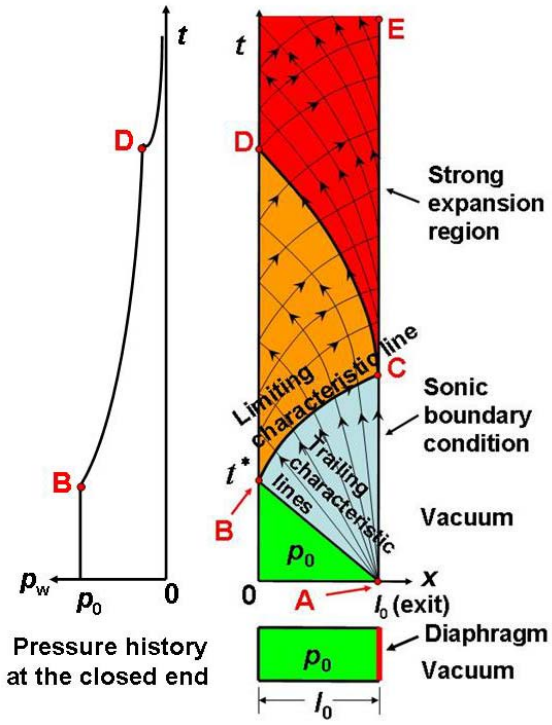

Fig. 1 The characteristic lines and closed-end-wall pressure history (without the extension tube).

is constant at $p = p_0$, analogous to the so-called plateau pressure observed in detonation tubes. After the expansion wave reflected at the closed end, the closed end pressure begins to decay. The pressure ratio between the inside and outside of the tube is essentially infinite so that the shock tube exit velocity can be assumed to be the sound velocity. Hence, the characteristic line is vertical to x-axis at the shock tube exit (the line AE in Fig.1).

The left-propagating expansion wave is reflected at the closed end for $t > t^*$ and a right propagating wave is generated to maintain zero velocity at the closed end. The region BCD is the interaction region between leftward and rightward-moving expansion waves. Note that the region A0BDC is same in both cases with and without an expansion tube. The rightward moving waves in the region BCD reach the exit of the shock tube (the line EC in Fig.1) and are reflected toward the closed end. The sound-velocity boundary condition creates the strong expansion region CDE in Fig.1. This region results in discontinuity of the first derivative of the pressure history at the point D on the closed end of the tube. The pressure history at the closed end can be integrated by time and to compute the specific impulse

$$I = At^* p_0 + A\int_{t^*}^{\infty} p(t)dt \tag{1}$$

and the specific impulse can be calculated as

$$I_{sp} = \frac{I}{mg} = \frac{I}{\rho_0 l_0 Ag} \tag{2}$$

B. MOC Computation with Extension Tube

The x-t diagram of the characteristics curves and diagram of the closed-end wall pressure p_w history are shown in Fig 2. The diaphragm is ruptured at the time $t = 0$ as is the case with above, and the expansion wave propagates toward both the closed end and the exit of the extension tube. The region A0BDC in Fig. 2 is same as one in Fig. 1 (the case without extension tube). The expansion wave front on the right side (the leading characteristic line) propagates to the exit of the extension tube and the expansion wave front on the left side is reflected at the closed end. The flow velocity at the exit for this case is supersonic (greater than the sound velocity) and unlike the previous case, there are no reflected waves from the exit. The characteristic lines after the curve CD are fundamentally different from the lines of the case without the extension tube. As a consequence, the pressure after the time corresponding to the point D on the closed end decays more slowly than for the case without the extension tube. The slower pressure decay results in additional impulse compared to the case without the extension tube.

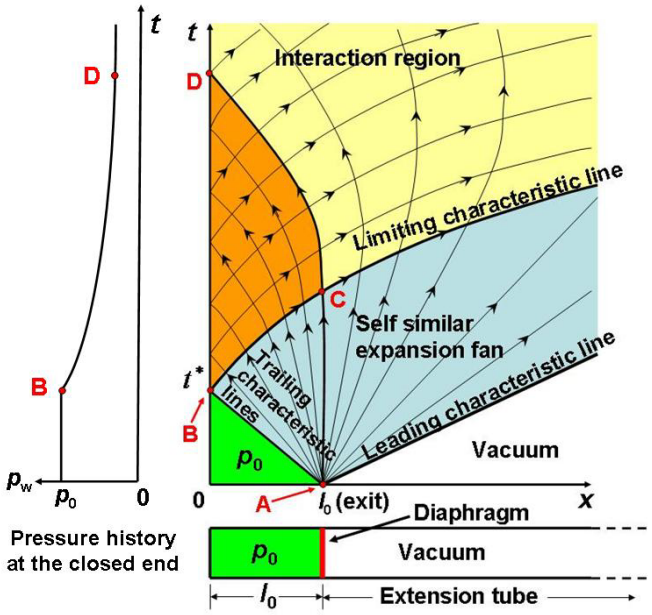

Fig. 2 The characteristic lines and closed-end-wall pressure history (with the extension tube).

The calculated characteristic lines for the case with the extension tube (0.6 m, nitrogen) are shown in Fig 3. The pressure history at the closed end is shown for cases with and without the extension tube (1.2 m) in Fig 4. The gas is nitrogen. The pressure histories are clearly identical up to the time corresponding to the point D and then the case with the expansion tube decays more slowly than the case without.

C. Scaling Analysis

The dependence of specific impulse on gas type and dimensions can be determined by applying simple ideas to evaluate the parameters in equation (1). The time $t^* = l_0/c_o$ where l_0 is the length of the driver section and c_o is the initial sound speed in the driver gas. Using the ideal gas relationships for sound speed and gas density, we can write the specific impulse in scaled form as

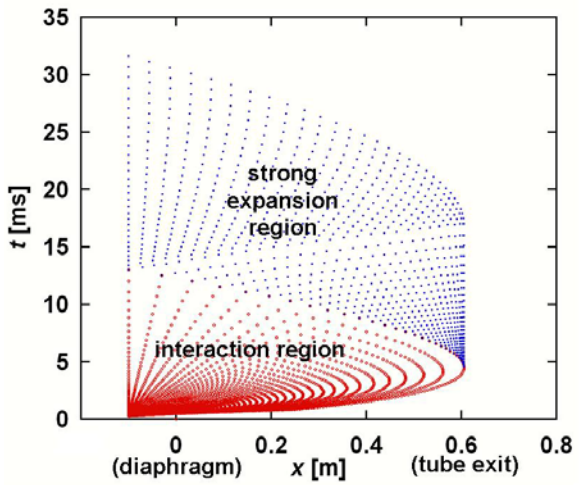

Fig. 3 Calculated characteristic lines for nitrogen with 0.6 m extension tube.

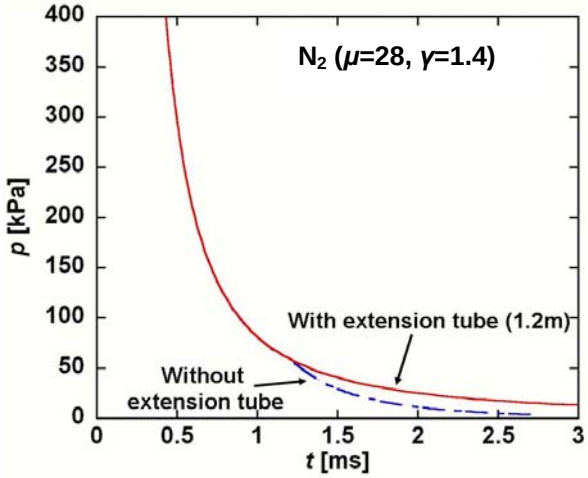

Fig. 4 Comparison of the closed-end wall pressure histories for cases with and without the extension tube.

$$I_{\mathrm{sp}} = \frac{I}{mg} = I_{\mathrm{sp}}^{*} F(\gamma, L), \quad I_{\mathrm{sp}}^{*} = \frac{1}{g}\sqrt{\frac{\Re T_0}{\gamma\mu}} \tag{3}$$

where L is the total length of the shock tube and extension, see equation (8). The quantity I_{sp}^{*} represents the contribution to the impulse of the plateau period alone. The non-dimensional function F is given by

$$F = 1 + \int_{1}^{\infty} \frac{P(t/t^{*})}{P_0} d(t/t^{*}) \tag{4}$$

and the value of F-L represents the relative contribution of the decaying tail of the thrust wall pressure history to the impulse. Values of the time t^{*} and the impulse scaling parameter I_{sp}^{*} are given in Table 1.

III. Experimental Facility

The experimental apparatus is shown in Fig. 5. The shock tube and attached extension tube are attached to the frame that is suspended at four points by wires 0.601 m from the top of the vacuum chamber, as shown in Fig 6. The inner diameter of the shock tube is 39.5 mm and the length is 101.6 mm. The driver section (the shock tube) was sealed by a polyethylene-terephthalate plastic diaphragm (thickness of 100 μm) separating the driver section and driven section (the extension tube). A pneumatically-activated cutter ruptures the diaphragm. We use extension tubes of length l = 100 mm, 302 mm, 595 mm, 915 mm, and 1219 mm. Based on the volume, this results in fill fractions between 7.8% and 100%. We also tested the case without an extension tube (l = 0 m). The vacuum chamber had an inner diameter of 1.2 m, a length of 2 m, and an approximate internal volume of 2300 L.

We measure the pressure history at the closed end using a piezoelectric pressure gauge connected to a digital oscilloscope through an amplifier. The horizontal displacement of the shock tube is measured with a laser displacement sensor. We also use a video camera for recording the displacement of the shock tube and observing the motion to ensure that the pendulum is operating correctly.

The solenoid valve for filling the driver gas is attached at the bottom of the shock tube. A feed-through flange is located on the top of the vacuum chamber. The tubing and the electrical cables are brought upward to the shock tube. In the impulse calculation, we ignore the mass of the wires, tubes, and cables.

IV. Determining Specific Impulse

We determined the impulse from the experimental value of the maximum horizontal displacement by treating the suspended detonation tube as a loss-less pendulum and applying the conservation of energy to obtain the standard formula

$$\bar{I} = m\overline{v_0} = m\sqrt{2g(l_w - \sqrt{l_w^2 - \overline{\Delta x_{max}}^2})} \tag{5}$$

In this equation, I is the measured impulse, m is the pendulum mass, v_0 is equivalent initial velocity of the shock tube just after the gas was exhausted, l_w is the suspension wire length, g is gravitational acceleration, and Δx is the maximum horizontal displacement. The specific impulse I_{sp} is calculated by dividing the impulse by the mass of driver gas and gravitational acceleration

$$\overline{I_{sp}}(l) = \frac{\bar{I}(l)}{\overline{m_g} g} \tag{6}$$

where m_g is the driver gas mass and l is length of extension tube. The symbol [—] denotes the experimental value. The mass of gas is computed from the measured temperature and pressure

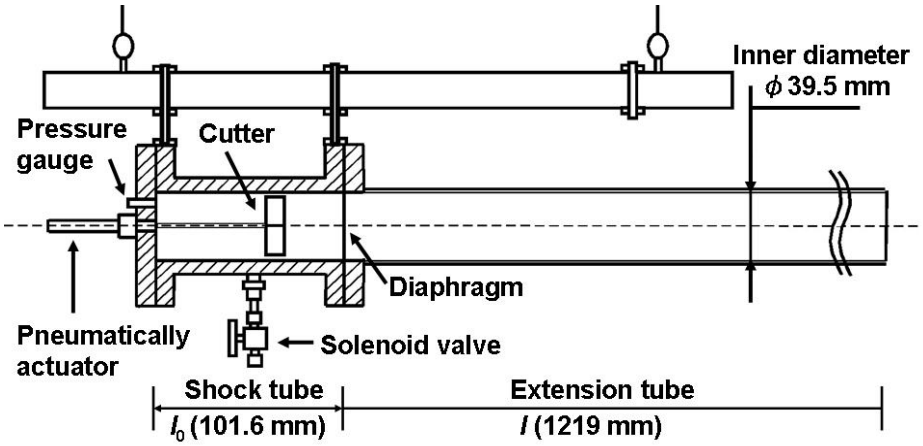

Fig. 5 Schematic diagram of the shock tube with an extension tube.

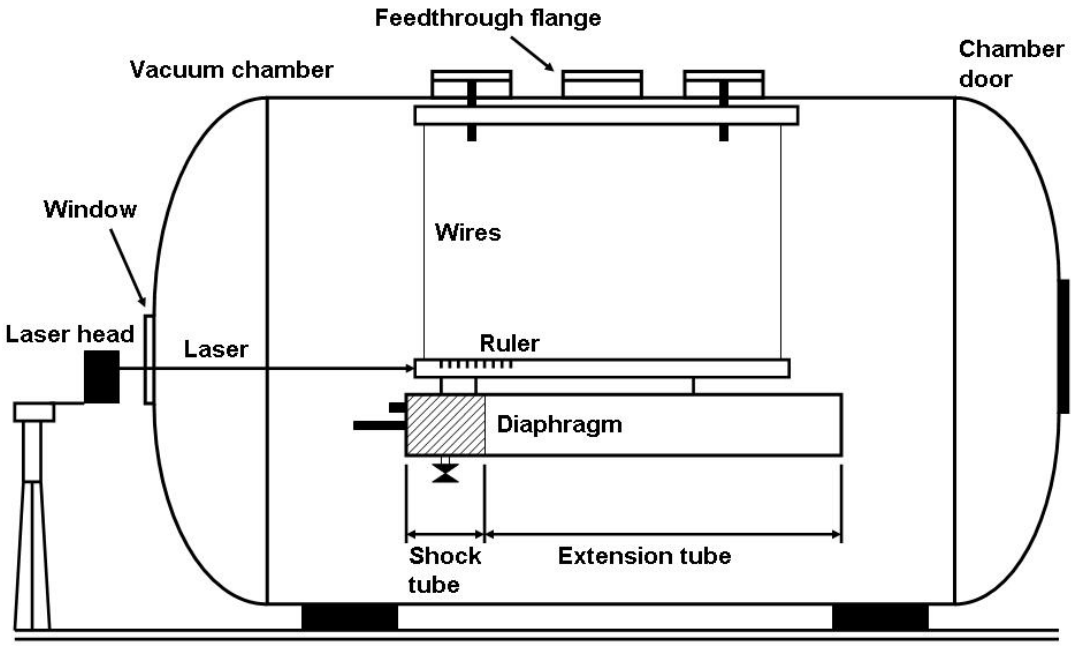

Fig. 6 Schematic diagram of the vacuum chamber showing mounting arrangement of shock tube.

$$\overline{m_g} = \overline{\rho_0} V = \frac{\overline{p_0} V \mu}{\Re \overline{T_0}} \tag{7}$$

where ρ_0 is initial fill density of the driver gas, p_0 is initial fill pressure, V is the volume inside the shock tube driver section, $\Re$ is the universal gas constant, and T_0 is initial temperature

V. Experimental Result and Analysis

A. Specific Impulse Measurement

Measurements of the specific impulse at various extension tube lengths for all gases are plotted in Fig 7. The results calculated by the method of characteristics are also shown in Fig. 7. The values of impulse shown in Fig. 7 were obtained from the measured maximum displacement as described in the previous section. We also calculated the initial velocity of the pendulum by differentiating the location history of the laser displacement sensor and obtained maximum displacement recorded by video camera. We obtained approximately same specific impulse from all three approaches. Within the observed experimental uncertainty, the calculated and experimental values are in reasonable agreement except for the hydrogen case, for which the computations are systematically higher.

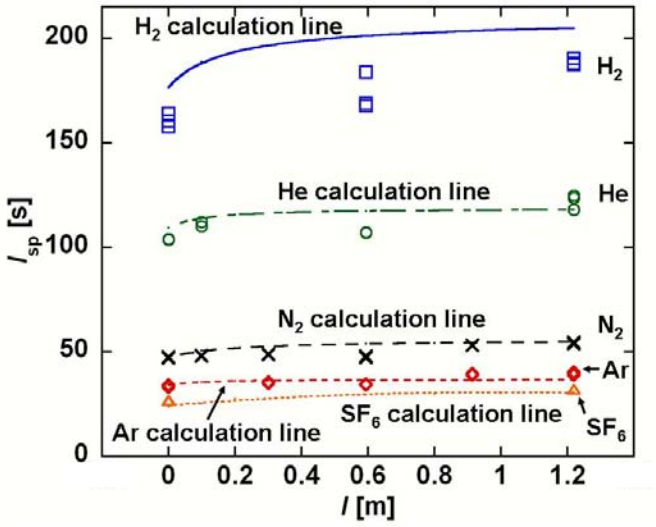

Fig. 7 Specific impulse of all gases as a function of the extension tube length.

We define a non-dimensional length L which is the total length of the shock tube plus extension divided by the length of the shock tube

$$L = \frac{l_0 + l}{l_0} \tag{8}$$

When L = 1, there is no extension tube; as $L \rightarrow \infty$, the extension tube is much larger than the driver section. In the present study, L_{max} = 13 (l_{max} = 1.22 m). The experimental values of scaled impulse $\bar{I}_{sp}(L)/I^*_{sp}$ are shown as a function of L in Fig 8. As anticipated from the MOC computations, the non-dimensional specific impulse clearly increases with increasing extension length. The magnitude of the effect is an increase of specific impulse of about 20% (see Table 2) between no extension and the maximum length extension studied in the present tests. The dramatic increase in specific impulse with decreasing molar mass is almost completely accounted for by the variations in sound speed and density as given by the scaling relationship equation (3). The actual impulses are in the inverse order in magnitude as compared to the specific values.

Table 2. Comparison of measured specific impulse with (1.22 m) and without the extension tube.

	Ar	He	N_2	H_2	SF_6
$\bar{I}_{sp}(1.22)/\bar{I}_{sp}(0)$	1.177	1.177	1.144	1.190	1.200

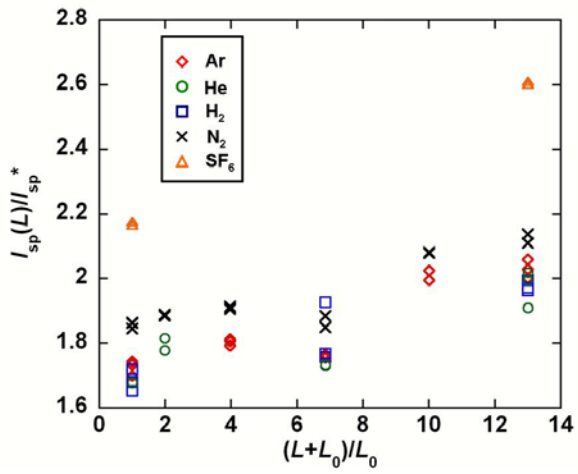

Fig. 8 Measured non-dimensional specific impulse $\bar{I}_{sp}(L)/I^*_{sp}$ for all gases as a function of non-dimesional length *L*.

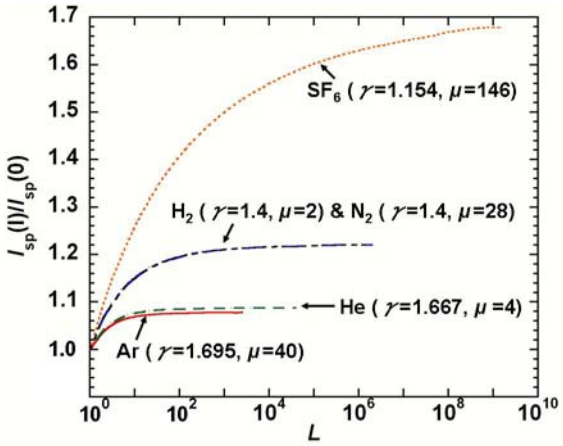

Fig. 9 Computed non-dimensional specific impulse $I_{sp}(l)/I_{sp}(0)$ Vs nondimesional length *L*.

During the one-dimensional expansion process the thermal energy of the gas is converted to uni-directional kinetic energy. Molecules like SF_6 with a large number of degrees of freedom (smaller specific heat ratios) will have greater final kinetic energies than molecules with a small number of degrees of freedom like He and Ar. In the limit of an unsteady expansion to zero pressure, unsteady gas dynamics of a perfect gas predicts that the final gas velocity will be

$$u_\infty = \frac{2}{\gamma - 1} c_0 \tag{9}$$

This suggests that for the same length extension tube, we expect that a lower specific-heat-ratio gas will have a greater specific impulse $I_{sp}(l)/I_{sp}(0)$. This is confirmed by the computational results shown in Figure 9 which shows that for extraordinarily long extension tubes an effect of specific heat ratio should be observed. However, as the present experiment results show, for extension tubes on the order of 10-100 times the driver length, only a modest effect of specific heat ratio is expected. These computations overestimate the effect since, in real gases, "freezing" of the energy exchange processes is expected to occur as the collision rate decreases in the very low pressure gas at the front of the expansion wave. Given the scatter in the present results and the limited range of extension tube lengths, it is not possible to draw any definite conclusions about these effects.

B. Diaphragm Effect and Pressure Profile in Driver Section

We carried out some experiments with ambient atmosphere pressure to examine the effect of diaphragm thicknesses of 25 μm, 50 μm, and 75 μm. The driver section was filled with helium and the diaphragm was ruptured by bursting rather than using the cutter. An extension tube was added to the driver (Fig. 10) so that the pressure history could be measured at four locations: 75.4 mm, 150.8 mm, 226.2 mm, and 301.6 mm (closed end) from exit (open end). A representative example of pressure history for the case of using 25μm diaphragm without an extension

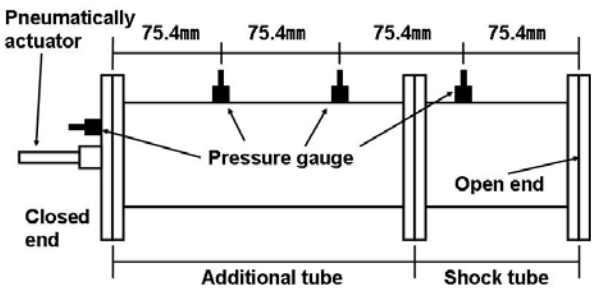

Fig. 10 Schematic diagram of shock tube and additional tube with pressure gauge ports.

tube is shown in Figure 11. We can clearly observe the propagation of the head of the expansion wave toward the closed end. Thinner diaphragms resulted in more rapid development of the expansion wave.

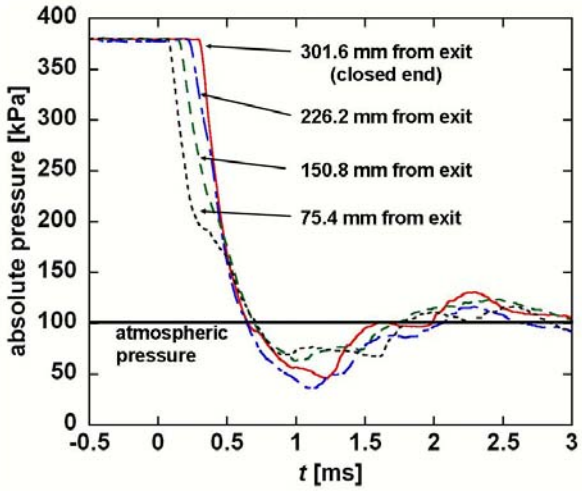

Fig. 11 Pressure history in atmospheric pressure operation using the 25 μm thick diaphragm.

VI. Conclusions

The goal of this study was to examine, through the shock tube analogy, the possibility of using the partial fill effect to improve pulsed detonation engine performance for space applications. Our tests and numerical simulations demonstrate a modest specific impulse increase with extension tube length in vacuum operation. The longest extension tube (fill fraction of 7.8%), results in an increase of 18% in specific impulse for helium and argon driver gases, 14.4% for nitrogen, 19% for hydrogen, and 20% for sulfur hexafluoride. The observed increase in specific impulse is due to the wave propagation processes in the gas that has expanded into the extension tube. Computations and measurements show that the secondary expansion waves created when the main expansion reaches the open end of the tube are what limit the actual impulse values. The mechanism of impulse enhancement is the slower rate of pressure decay due to one-dimensional wave propagation with a long extension tube compared to the three-dimensional expansion at the open end. The partial fill effects observed with shock tube operation in a vacuum are much smaller than the increases that are observed when operating a detonation tube with partial fill at ambient pressures.

Acknowledgments

This experiment was carried out by using the vacuum chamber in the low-density wind tunnel experimental laboratory, JAXA/ISAS. This work was supported by Grant-in-Aid for Scientific Research, Young Researchers (B) (17760633), "Study of High I_{sp} Pulse Detonation Rocket by Intermittent Expansion Thrust Enhancement Effect," Ministry of Education, Culture, Sports, Science and Technology. JES's stay at Tsukuba University was funded by a Japan Society for the Promotion of Science, Invitation Fellowship for Research.

References

[1]Roy, G. D., Frolov, S. M., Borisov, A. A., and Netzer, D. W., "Pulse detonation propulsion: challenges, current status, and future perspective," *Prog. Energy Combust. Sci.*, Vol. 30, 2004, pp. 545-672.

[2]Zhdan, S. A., Mitrofanov, V. V., and Sychev, A. I., "Reactive Impulse from the Explosion of a Gas Mixture in a Semi-infinite Space," *Combustion, Explosion and Shock Waves*, Vol. 30, No. 5, 1994, pp. 657-663.

[3]Zitoun, R. and Desbordes, D., "Prospective Performances of Pulsed Detonations," *Comb. Sci. Tech.*, Vol. 144, No. 1, 1999, pp. 93-114.

[4]Falempin, F., Bouchaud, D., Forrat, B. Desbordes, D., and Daniau, E., "Pulsed Detonation Engine Possible Application to Low Cost Tactical Missile and to Space Launcher," 37th AIAA/ASME/SAE/ASEE Joint Propulsion Conference and Exhibit, July 8-11, 2001, Salt Lake City, UT, AIAA, 2001-3815.

[5]Cooper, M., and Shepherd, J. E., "The Effect of Nozzle and Extensions on Detonation Tube Performance," AIAA 2002-3628, 38th AIAA/ASME/SAE/ASEE Joint Propulsion Conference and Exhibit, July, 2002, Indianapolis.

[6]Cooper, M. A., *Impulse Generation by Detonation Tubes*, Ph.D. thesis, California Institute of Technology, Pasadena, California, May 2004.

[7]Cooper, M., Shepherd, J. E., and Schauer, F., "Impulse correlation for partially-filled tubes," *Journal of Propulsion and Power*, Vol. 20, No. 5, 2004, pp. 947-950, (Preprint – see journal for final version).

[8]Li, C. and Kailasanath, K., "Performance Analysis of Pulse Detonation Engines with Partial Fuel Filling," *Journal of Propulsion and Power*, Vol. 19 (5), 2003, pp. 908-916.

[9]Kasahara, J., Arai, T., and Matsuo, A., "Experimental Analysis of Pulse Detonation Engine Performance by Pressure and Momentum Measurements," AIAA 03-0893.

[10]Endo, T., Kasahara, J., Matsuo, A., Inaba, K., Sato, S., and Fujiwara, T., "Pressure History at the Thrust Wall of a Simplified Pulse Detonation Engine," *AIAA Journal*, Vol. 42, No. 9, September, 2004, pp. 1921-1930.

[11]Kasahara, J., Tanahashi, Y., Hirano, M., Numata, T., Matsuo, A., and Endo, T., "Experimental Investigation of Momentum and Heat Transfer in Pulse Detonation Engine," AIAA 04-0869.

[12]Sato, S., Matsuo, A., Endo, T., and Kasahara, J., "Numerical Studies on Specific Impulse of Partially Filled Pulse Detonation Rocket Engines," *Journal of Propulsion and Power*, Vol. 22, No. 1, 2006, pp. 64-69.

[13]Endo, T., Yatsufusa, T., Taki, S., Matsuo, A., Inaba, K., and Kasahara, J., "Homogeneous-Dilution Model of Partially Fueled Simplified Pulse Detonation Engines," *Journal of Propulsion and Power*, Vol. 23, No. 5, September-October, 2007, pp. 1033-1041.

[14]Kasahara, J., Tanahashi, Y., Numata, T., Matsuo, A., and Endo, T., "Experimental Studies on L/D Ratio and Heat Transfer in Pulse Detonations," 19th International Colloquium on the Dynamics of Explosion and Reactive Systems, Paper 65, July-August, 2003.

[15]Radulescu, M. I., and Hanson, R. K., "Effect of Heat Loss on Pulse-Detonation-Engine Flow Fields and Performance," *Journal of Propulsion and Power*, Vol. 21 (2), 2005, pp. 908-916.

[16]Cooper, M., Jackson, S., Wintenberger, E., and Shepherd, J. E., "Direct Experimental Impulse Measurements for Detonations and Deflagrations," *Journal of Propulsion and Power*, Vol. 18, 2002, 1033-1041.

[17]Cooper, M., and Shepherd, J. E., "Detonation Tube Impulse in Subatomospheric Environments," *Journal of Propulsion and Power*, Vol. 22, No. 4, 2006, pp. 845-851.

[18]Morris, C. I., "Numerical Modeling of Single-Pulse Gasdynamics and Performance of Pulse Detonation Rocket Engines," *Journal of Propulsion and Power*, Vol. 21, 2005, pp. 527-538.

[19]Matsuo, K., *Compressible Flow Dynamics*, Rikogakusha Publishing, 1994, pp. 200-233.

[20]Japan Society of Mechanical Engineers, *Flow Thermophysical Properties*, 1983.